

# Reliability of Coupled Oscillators II: Larger Networks

Kevin K. Lin<sup>1</sup>, Eric Shea-Brown<sup>1,2</sup>, and Lai-Sang Young<sup>1</sup>

<sup>1</sup> Courant Institute of Mathematical Sciences,

<sup>2</sup> Center for Neural Science

New York University, New York, NY 10012, U.S.A.

August 22, 2007

## Abstract

We study the *reliability* of phase oscillator networks in response to fluctuating inputs. Reliability means that an input elicits essentially identical responses upon repeated presentations, regardless of the network's initial condition. In this paper, we extend previous results on two-cell networks to larger systems. The first issue that arises is chaos in the absence of inputs, which we demonstrate and interpret in terms of reliability. We give a mathematical analysis of networks that can be decomposed into modules connected by an acyclic graph. For this class of networks, we show how to localize the source of unreliability, and address questions concerning downstream propagation of unreliability once it is produced.

## Contents

<b>Introduction</b>	<b>2</b>
<b>1 Model and measure of reliability</b>	<b>3</b>
1.1 Coupled phase oscillator systems . . . . .	3
1.2 Lyapunov exponents as indicator of reliability . . . . .	4
<b>2 Intrinsic network chaos</b>	<b>6</b>
2.1 Chaotic behavior in undriven networks . . . . .	6
2.2 Suppression of network chaos by inputs: a case study . . . . .	7
<b>3 Acyclic networks and modular decompositions</b>	<b>9</b>
3.1 Skew-product representation of acyclic networks . . . . .	9
3.2 Lyapunov exponents of acyclic networks . . . . .	11
3.3 Modular decompositions and quotient systems . . . . .	13

<b>4 Propagation of unreliability</b>	<b>14</b>
4.1 Measuring reliability at individual network sites . . . . .	14
4.2 Sites downstream from unreliable modules . . . . .	16
<b>5 Examples: reliability and unreliability in small networks</b>	<b>18</b>
5.1 The $N$ -ring . . . . .	18
5.2 2-loops driving 2-loops . . . . .	19
<b>6 Modules in isolation versus as part of larger system</b>	<b>21</b>
<b>7 An illustrative example</b>	<b>24</b>
<b>Conclusions</b>	<b>26</b>

## Introduction

This is a sequel to *Reliability of Coupled Oscillators I* [21], but can be read independently (if the reader is willing to take a few facts for granted). Both papers are about the reliability of coupled oscillator networks in response to fluctuating inputs. Reliability here refers to whether a system produces identical responses when it is repeatedly presented with the same stimulus. The context in this paper is that of heterogeneous networks of coupled phase oscillators. The stimuli, or input signals, are assumed to be white noise; they are received by some components of the network and relayed to others with or without feedback.

There has been substantial progress in understanding the reliability of single oscillators [30, 25, 45, 37, 33, 28, 17, 8, 9]. Paper I contains a detailed study of reliability properties for the simplest possible network, that of two coupled cells [21]. We showed that this small network displays both reliable and unreliable behaviors in broad parameter ranges. Here, we consider larger networks building on some of the insight gained from Paper I.

Our first observation concerns intrinsic network chaos, meaning the network in question can be chaotic even in the absence of any inputs. This phenomenon occurs only in systems consisting of 3 or more oscillators, and the chaos can be sustained in time and ubiquitous in the phase space. Its implications are discussed in Sects. 2 and 6.

Our main technical analysis is in Sect. 3. It is first carried out for acyclic networks, that is, networks whose coupling connections have no cycles, and then extended to a larger class obtained by replacing the nodes in acyclic networks by *modules* (which are themselves networks). It is at this latter class that much of the discussion in the rest of the paper is aimed.

In a larger network, there is a need to understand the problem locally as well as globally: when unreliability occurs, it is useful to know where it is created and which parts of the network are affected. Therefore, instead of solely using a single index, namely the largest Lyapunov exponent  $\lambda_{\max}$ , as indicator of reliability for the entire system, we have sought to localize the source of unreliability, and to devise ways to assess the reliability of outputs registered at any given site. Among our findings is that once produced, unreliability propagates; no site downstream can then be completely reliable.

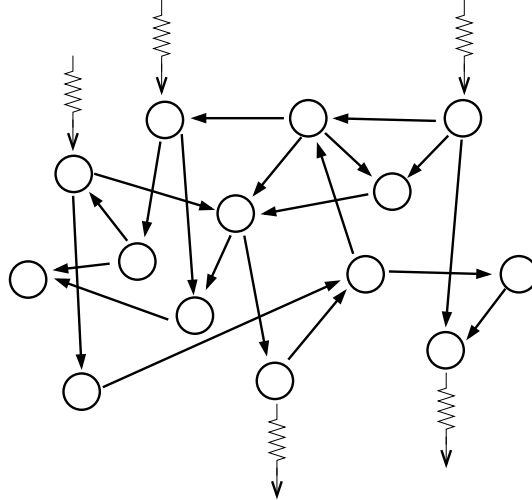


Figure 1: Schematic of a forced oscillator network.

In studying networks that decompose into smaller modules, there is a reassembly issue, namely how the information gained from studying the modules separately can be leveraged in the analysis of the full network. We will present some evidence to show that such a strategy may be feasible.

Numerous examples are given to illustrate the ideas proposed. In addition to the 2-oscillator system studied in [21], we present a few other examples of small networks capable of both reliable and unreliable behavior, finding some rather curious (and unexplained) facts along the way.

The mathematical analysis in Sect. 3 is rigorous, as are the facts reviewed in Sects. 2.2 and 4.1. The rest of the investigation is primarily numerical, supported whenever possible by facts from dynamical systems theory. In the course of the paper we have highlighted a number of observations, based in part on empirical data, that are directly relevant for the broader theoretical questions at hand.

There is a vast literature on networks of oscillators; it is impossible to give general citations without serious omissions. We have limited our citations to a sample of papers and books with settings closer to ours or which treat specifically the topic of reliability (see below). We mention in particular the recent preprint [36], which discusses the reliability of large, sparsely coupled networks in a way that complements ours.

## 1 Model and measure of reliability

### 1.1 Coupled phase oscillator systems

We consider in this paper networks of coupled phase oscillators in the presence of external stimuli. A schematic picture of such a setup is shown in Figure 1. The networks considered are of the type that arise in many settings; see *e.g.*, [30, 34, 19, 14, 42, 32, 3, 5, 7].

The *unforced* systems, *i.e.*, the systems without external stimuli, are described by

$$\dot{\theta}_i = \omega_i + z(\theta_i) \sum_{j \neq i} a_{ji} g(\theta_j), \quad i = 1, \dots, N. \quad (1)$$

In this paper,  $N$  can be any number  $\geq 1$ ; in particular, it can be arbitrarily large. The state of oscillator  $i$  is described by an angular variable  $\theta_i \in S^1 \equiv \mathbb{R}/\mathbb{Z}$ ,  $i = 1, \dots, N$ . Its intrinsic frequency is given by a constant  $\omega_i$ . We allow these frequencies to vary from oscillator to oscillator. The second term on the right represents the coupling:  $a_{ji} \in \mathbb{R}$ ,  $g$  is a “bump function” vanishing outside of a small interval  $(-b, b)$ ; on  $(-b, b)$ , it is smooth,  $\geq 0$ , and satisfies  $\int_{-b}^b g(\theta) d\theta = 1$ ;  $z(\theta)$  is a function which in this paper is taken to be  $z(\theta) = \frac{1}{2\pi}(1 - \cos(2\pi\theta))$ . The meaning of this coupling term is as follows: We say the  $j$ th oscillator “spikes” when  $\theta_j(t) = 0$ . Around the time that an oscillator spikes, it emits a pulse which modifies some of the other oscillators [29, 35, 13, 27]. The sign and magnitude of  $a_{ji}$  describe how oscillator  $j$  affects oscillator  $i$ :  $a_{ji} > 0$  (resp.  $a_{ji} < 0$ ) means oscillator  $j$  excites (resp. inhibits) oscillator  $i$  when it spikes, and  $a_{ji} = 0$  means oscillator  $i$  is not directly affected. In this paper,  $b$  is taken to be about  $\frac{1}{20}$ , and the  $a_{ji}$  are taken to be  $\mathcal{O}(1)$ . Finally, the function  $z(\theta)$ , often called the phase response curve [41, 11, 6, 19], measures the variable sensitivity of an oscillator to coupling and stimulus inputs.

The *stimulus-driven* systems are of the form

$$d\theta_i = \omega_i dt + z(\theta_i) \left( \sum_{j \neq i} a_{ji} g(\theta_j) dt + I_i(t) \right),$$

$$I_i(t) = \varepsilon_i dW_i(t), \quad i = 1, \dots, N. \quad (2)$$

Here,  $I_i(t)$  is the external stimulus received by oscillator  $i$ ; it is taken to be white noise with amplitude  $\varepsilon_i$ . For simplicity, we assume that for  $i \neq j$ ,  $dW_i(t)$  and  $dW_j(t)$  are either independent, or they are one and the same, *i.e.*, the same input is received by both oscillators although the amplitudes may differ. As discussed earlier, we are primarily interested in situations where inputs are received by only a subset of the oscillators, with  $\varepsilon_i \approx 0$  for the rest. Likewise, we are sometimes interested in the response registered at only a subset of the oscillators rather than the whole network. See Fig. 1.

For more on the motivation and interpretation of this model, see Sect. 1.2 of [21].

## 1.2 Lyapunov exponents as indicator of reliability

*Reliability* in this paper refers to the following: Suppose the stimuli in Eq. (2) described by the terms  $\varepsilon_i I_i(t)$  are turned on at time  $t = 0$ . Will the response of the system depend on the initial state of the system when the stimuli are presented? That is to say, let  $\Theta(t)$  be the solution of Eq. (2). To what degree does  $\Theta(t)$  depend on  $\Theta(0)$  after some initial period of adjustment? If the dependence on  $\Theta(0)$  is negligible after a transient, we think of the system is *reliable*; and if different  $\Theta(0)$  lead to persistently different responses at time  $t$  for all or most  $t$ , we say the system is *unreliable*. Needless to say, the lengths of the transient and the degree to which the responses differ are important in practical situations, but these issues will not be considered here.

The measure of reliability used in a good part of this paper is  $\lambda_{\max}$ , the largest Lyapunov exponent of the system. We briefly recall here the meaning of this number and its relation to reliability as discussed above, referring the reader to [1, 2] for background material on stochastic flows and to Sect. 2 of [21] for a more detailed discussion of how this material is used in the study of reliability.

We view Eq. (2) as a stochastic differential equation (SDE) on  $\mathbb{T}^N \equiv S^1 \times \cdots \times S^1$  with phase variables  $(\theta_1, \dots, \theta_N)$ . A well known theorem gives the existence of a *stochastic flow of diffeomorphisms*. That is to say, for almost every realization  $\omega$  of white noise, there exist flow maps of the form  $F_{t_1, t_2; \omega}$ : here  $t_1 < t_2$  are any two points in time, and  $F_{t_1, t_2; \omega}(\Theta(t_1, \omega)) = \Theta(t_2, \omega)$  where  $\Theta(t, \omega)$  is the solution of (2) corresponding to  $\omega$ . By the Lyapunov exponents of Eq. (2), we refer to the Lyapunov exponents of  $F_{0, t; \omega}$  as  $t$  increases. These numbers do not depend on  $\omega$ ; and they do not depend on  $\Theta(0)$  if Eq. (2) is ergodic (which it often is). The largest Lyapunov exponent is denoted by  $\lambda_{\max}$ .

In [21], cf. [33, 9, 17], we used of  $\lambda_{\max}$  as a measure of reliability. Specifically,  $\lambda_{\max} < 0$  is equated with reliability,  $\lambda_{\max} > 0$  represents unreliable behavior, and  $\lambda_{\max} = 0$  is inconclusive.<sup>1</sup> These criteria will continue to be used in this paper.

To understand why  $\lambda_{\max}$  is a reasonable indicator of reliability, recall the idea of *sample measures*: if we let  $\mu$  denote the stationary measure of (2), *i.e.* the stationary solution to the Fokker-Planck equation, the sample measures are then the conditional measures of  $\mu$  given the past history of the stimuli. More precisely, if we think of  $\omega$  as defined for all  $t \in (-\infty, \infty)$  and not just for  $t > 0$ , then  $\mu_\omega$  describes what one sees at  $t = 0$  given that the system has experienced the input defined by  $\omega$  for all  $t < 0$ . Sample measures thus give an approximation of what one sees in response to an input presented on a time interval  $[-t_0, 0)$  for large enough  $t_0 > 0$ . If we let  $\sigma_t$  denote the time-shift of the Brownian path  $\omega$ , then sample measures evolve in time according to  $(F_{0, t; \omega})_* \mu_\omega = \mu_{\sigma_t \omega}$ . As explained in [21], if stimuli corresponding to a realization  $\omega$  are turned on at  $t = 0$ , then  $\mu_{\sigma_t \omega}$  gives a good approximation of the responses of the system at sufficiently large times  $t$  for an ensemble of initial conditions sampled from a smooth density. In particular, if  $\mu_{\sigma_t \omega}$  collapses down to a single point as  $t$  increases, then we conclude that initial conditions have little effect after transients, *i.e.* the system is reliable. If  $\mu_{\sigma_t \omega}$  is spread out nontrivially in the phase space, and this condition persists with  $t$ , then we conclude that different initial conditions have led to different responses at time  $t$ , which is exactly what it means for the system to be unreliable.

The relation between sample measures, which represent a collection of the system's possible responses, and  $\lambda_{\max}$ , its top Lyapunov exponent, is summarized in the following general result from dynamical systems theory.

**Theorem 1.** *Consider a SDE with an ergodic stationary measure  $\mu$ .*

- (1) [16] *If  $\lambda_{\max} < 0$ , then with probability 1,  $\mu_\omega$  is supported on a finite set.*
- (2) [20] *If  $\mu$  has a density and  $\lambda_{\max} > 0$ , then with probability 1,  $\mu_\omega$  is a random SRB measure.*

Case (1) is often referred to as the system having *random sinks*. When  $\lambda_{\max} < 0$ , in the vast majority of situations  $\mu_\omega$  is supported on a single point; we therefore equate it with reliability as in,

---

<sup>1</sup>We note that there are other ways to measure unreliability which seem to us to be equally reasonable. For example, one can take the sum of all *positive* Lyapunov exponents.

e.g., [33, 28]. In Case (2), the system is said to have a *random strange attractor*. For deterministic systems, SRB measures are well studied objects with a distinctive geometry: they have densities on (typically) lower dimensional surfaces that wind around the phase space in a complicated way; see [4]. Here we have a random (*i.e.*  $\omega$ -dependent) version of the same picture. Thus the resulting geometry is a readily recognizable signature of unreliability.

Finally, we remark that  $\lambda_{\max}$  is a *global* indicator of unreliability, meaning a positive exponent will tell us only that the network possesses some unreliable degrees of freedom: it does not specify where this unreliability is produced, whether its effects are localized, and so on. Different measurements are needed to answer these more refined questions. They are discussed in Sects. 3–6.

## 2 Intrinsic network chaos

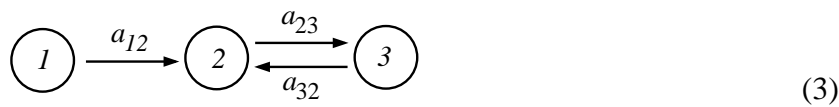
### 2.1 Chaotic behavior in undriven networks

This section discusses an issue that did not arise in [21]. Our criterion for unreliability,  $\lambda_{\max} > 0$ , is generally equated with *chaos*. In the 2-oscillator network studied in [21], this chaotic behavior is triggered by the input: without this forcing term, the system cannot be chaotic as it is a flow on a two-dimensional surface. The situation is quite different for larger networks.

**Observation 1:** *Networks of 3 or more pulse-coupled phase oscillators can be chaotic in the absence of any external input.*

We begin by explaining what we mean by “chaotic.” It is well known that systems of 3 or more coupled oscillators without external input can have complicated orbits, such as homoclinic orbits or horseshoes (see, *e.g.*, [31, 27], and also [12, 5] for general references). These special orbits by themselves do not necessarily constitute a seriously chaotic environment, however, for they are not always easily detectable, and when horseshoes coexist with sinks, the chaotic behavior seen is transient for most choices of initial conditions. We claim here that networks with 3 or more oscillators can support a stronger form of chaos, namely that of *strange attractors*. There is no formal definition of the term “strange attractors” in rigorous dynamical systems theory. An often used characterization is the existence of SRB measures or physical measures, which describe the long-time distribution of orbits starting from positive Lebesgue measure sets of initial conditions [4, 43, 44]. At a minimum, one would insist that positive Lyapunov exponents be observed for almost all – or at least on a large positive Lebesgue measure set – of initial conditions. (In the case of horseshoes coexisting with sinks, for example, Lyapunov exponents for most initial conditions are negative after a transient.) In numerical simulations, one has to settle for positive Lyapunov exponents that are sustained over time for as many randomly chosen initial conditions as possible. This will be our operational definition of *intrinsic network chaos*.

One of the simplest configurations that support intrinsic network chaos is



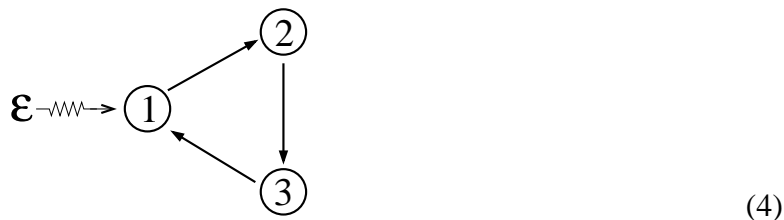
The setup above is similar to that studied in [21], except that the (2,3)-subsystem is kicked *periodically* by pulses from oscillator 1 rather than driven by an external stimulus in the form of white noise. Ignoring the presence of oscillator 1 for the moment, we saw in [21], Sect. 4.2, that when  $a_{23}$  and  $a_{32}$  are roughly comparable and away from 0, the phase space geometry of oscillators 2 and 3 is favorable for *shear-induced chaos*, a geometric mechanism for producing chaotic behavior. Indeed, a rigorous theory of this mechanism gives the existence of strange attractors with SRB measures when such a system is periodically kicked — provided the kicks are suitably directed and time intervals between kicks are sufficiently large [39, 40]. Even though the kick intervals (of  $\approx 1$ ) here are too short for rigorous results to be applicable, numerical simulations show that there are definitively positive exponents sustained over long periods of time when  $a_{12}$  is large enough.

As an example, consider system (3) with  $\omega_1, \omega_2, \omega_3 = 0.93, 1, 1.1$ , and  $a_{23}, a_{32} = 1, 1.45$ . We find that  $\lambda_{\max}$  increases from about 0.025 to 0.12 for  $a_{12} \in (1, 1.5)$ .<sup>2</sup> Notice that the system parameters above are chosen so that the (2,3)-subsystem is unreliable, that is, so that  $\lambda_{\max} > 0$  when oscillator 2 receives a white noise stimulus: see [21], Fig. 12. It is, after all, the same mechanism, namely shear-induced chaos, that produces the chaos in both situations. See [22], Study 4, for similar findings.

While there are certainly large classes of networks that do not exhibit intrinsic network chaos (*e.g.* see Sect. 3), from the example above one would expect that such chaos is commonplace among larger networks. Moreover, for intrinsically chaotic networks, one would expect  $\lambda_{\max}$  to remain positive when relatively weak stimuli are added to various nodes in the network. We have, in fact, come across a number of examples in which  $\lambda_{\max}$  remains positive for larger stimulus amplitudes. This raises the following issue of interpretation: In an intrinsically chaotic network that also displays  $\lambda_{\max} > 0$  in the presence of inputs, it is unclear how to attribute the source of unreliability, since the effects of inputs and intrinsic chaos are largely inseparable. We adopt here the view that whatever the cause, such a network is unreliable.

## 2.2 Suppression of network chaos by inputs: a case study

An interesting question is whether or not networks with intrinsic chaos of the form described above, *i.e.* with  $\lambda_{\max} > 0$  for large sets of initial conditions in the absence of inputs, necessarily respond unreliably to external stimuli. We find that the answer is “no”: we have come across a number of instances where weakly chaotic networks are stabilized by sufficiently strong inputs. An example is in the following 3-cell ring:



We find small regions of parameter space near  $a_{12} = 1, a_{23} = 2, a_{31} = 0.6$  with intrinsic network

<sup>2</sup>These Lyapunov exponents are computed starting from  $\sim 10$  initial conditions and have an absolute error of roughly 0.005.

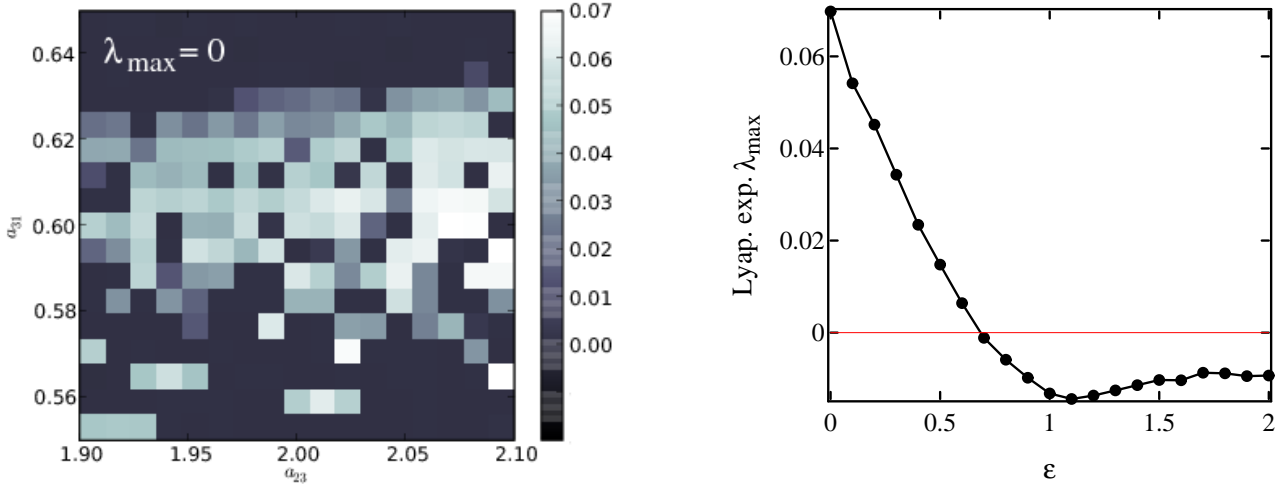


Figure 2: Suppression of intrinsic chaos in Eq. (10). **Left:** the Lyapunov exponent  $\lambda_{\max}$  with  $\epsilon = 0$  is shown as a function of  $a_{23}$  and  $a_{31}$  ( $a_{12}$  is fixed at 1). Each exponent is computed using 4 initial conditions. For the vast majority ( $\geq 95\%$ ) of the points computed, the error in the computed exponent is  $\lesssim 0.005$ . **Right:** we show the response to  $\epsilon > 0$  for  $a_{23} = 2.075$  and  $a_{31} = 0.6025$ . In all plots, we use  $\omega_1 = 1$ ,  $\omega_2 = 0.95$ , and  $\omega_3 = 1.1$ .

chaos, as evidenced by positive values of  $\lambda_{\max}$ : see Fig. 2(a). As the reader will notice,  $\lambda_{\max}$  oscillates quite wildly in this region, with  $\lambda_{\max} > 0$  and  $\lambda_{\max} = 0$  occurring at parameter values in close proximity. This is characteristic of a large class of *deterministic* dynamical systems as we now explain.

The phase space of system (4) is the 3-torus. Taking the section  $\{\theta_1 = 0\}$  of the  $\epsilon = 0$  flow, we obtain a return map  $\Psi$  from the 2-torus to itself. There are well known examples of maps of the 2-torus that are uniformly hyperbolic; a case in point is the “cat map”. These maps are robustly hyperbolic; it is impossible to destroy their positive Lyapunov exponents by reasonable-size perturbations. Our section map  $\Psi$ , however, cannot be of this type for topological reasons: it is not hard to see that  $\Psi$  can be deformed continuously to the identity map by suitably tuning system parameters. Generally speaking, for 2-D maps that can be deformed to the identity, the only way to form strange attractors is by “folding”. Such systems are at best *nonuniformly hyperbolic*; their observed Lyapunov exponents are the results of competing tendencies: there is expansion in the phase space, which necessarily leads to contraction elsewhere or in different directions, and the expanding and contracting directions are not separated as in the cat map. As a result of this competition, sustained, observable chaos, *i.e.*, strange attractors, live side by side in parameter space with transient chaos, *i.e.*, systems in which horseshoes and sinks coexist. The simplest family of examples exhibiting such a phenomenon is the logistic family [23, 15, 10]. This phenomenon also occurs in shear-induced chaos; see *e.g.*, [22]. For an exposition on nonuniformly hyperbolic systems, see *e.g.*, [43]. The mixed behavior alluded to above is discussed in, *e.g.* [44].

Thus even without explicit knowledge of the map  $\Psi$ , one would expect to see a pattern of behavior similar to that in Fig. 2(a) when positive exponents are present. Here,  $\lambda_{\max} = 0$  for the

flow corresponds to  $\Psi$  having a Lyapunov exponent  $\leq 0$ , including the parameters with transient chaos.

We now consider the effects of adding a stimulus, that is, taking  $\varepsilon > 0$  for system (4). Informally, one may think of the stimulus as sampling nearby parameters, averaging (in a loose sense) the different tendencies, with chaos suppression made possible by the presence of the mixed behavior. A sample of our numerical results is shown in Fig. 2(b). At  $\varepsilon = 0$ ,  $\lambda_{\max} > 0$ , indicating network chaos. As expected,  $\lambda_{\max}$  remains positive for small  $\varepsilon$ . But, as  $\varepsilon$  increases,  $\lambda_{\max}$  steadily decreases and eventually becomes mildly negative, demonstrating that sufficiently strong forcing can suppress intrinsic network chaos and make a network more reliable. A possible mechanistic explanation is that when  $\varepsilon$  is large enough, oscillator 1 is affected more by the stimulus than by oscillator 3 due to the relatively weak coupling  $a_{31}$ . As in the case of a single oscillator, the stimulus has a stabilizing effect on oscillator 1, making it reliable.

Our understanding from the discussion above may be summarized as follows:

**Observation 2:** *Some networks with weak intrinsic chaos will respond reliably to moderately strong stimuli.*

### 3 Acyclic networks and modular decompositions

Since the possibilities in completely general networks are vast, we think a good place to start may be the class of *acyclic* networks. These are networks in which there is a well defined direction of information flow. We will show that acyclic networks are not intrinsically chaotic, and they are never unreliable. Building on the analysis developed for acyclic networks, we identify a broader class that may be accessible to analysis, namely networks that admit a decomposition into modules with acyclic inter-module connections.

For simplicity, we assume throughout that the stimuli are independent; it is trivial to modify the results of this section to accommodate the situation when some of them are identical to each other.

#### 3.1 Skew-product representation of acyclic networks

We first describe the connection graph that corresponds to an oscillator network. Let each node of this graph,  $i \in \{1, \dots, N\}$ , correspond to an oscillator. Assign a directed edge from node  $i$  to node  $j$ ,  $i \neq j$ , if oscillator  $i$  provides input to oscillator  $j$ , *i.e.* if  $a_{ij} \neq 0$ ; in this case, we write  $i \rightarrow j$ . (For simplicity, we do not allow nodes to connect to themselves.) A *cycle* in such a directed graph is a sequence of nodes and edges  $i_1 \rightarrow i_2 \rightarrow \dots \rightarrow i_k \rightarrow i_1$  for some  $k > 1$ .

**Definition 3.1.** *We say an oscillator network is acyclic if its connection graph has no cycles.*

Given any pair of oscillators in an acyclic network, either they are “unrelated”, or one is “upstream” from the other. We say oscillator  $i$  is “upstream” from oscillator  $j$  if there is a sequence of nodes and edges that goes from  $i$  to  $j$ . The absence of cycles is precisely what makes this “upstream”–“downstream” notion well defined. We say oscillators  $i$  and  $j$  are “unrelated” if there

is no chain that goes from  $i$  to  $j$  or *vice versa*. Unrelated oscillators do not necessarily behave independently: they may, for example, receive input from the same source. Overall, the structures of acyclic networks can still be quite complex, with tree-like branching and recombinations possible.

Our first task is to find a systematic way to treat the dynamics within these networks.

**Lemma 3.1.** *In an acyclic graph, one can define for each node  $j$  a number  $m(j)$  representing its maximum number of ancestors, meaning*

- (i) *there is a chain of the form  $i_1 \rightarrow i_2 \rightarrow \dots \rightarrow i_{m(j)} \rightarrow j$ , and*
- (ii) *there is no chain of the form  $i_1 \rightarrow i_2 \rightarrow \dots \rightarrow i_{m(j)+1} \rightarrow j$ .*

The proof is simple: chains cannot be arbitrarily long without a node repeating, and such repeats are impossible in acyclic graphs.

Using the notation of Sect. 1.1, we now discuss the dynamical structure of acyclic oscillator networks. First, let  $\varphi_t$  denote the flow on  $\mathbb{T}^N$  in the absence of inputs, *i.e.*, with  $\varepsilon_i \equiv 0$ . We say  $\varphi_t$  *factors into a hierarchy of skew-products with 1-dimensional fibers* if after a permutation of the names of the  $N$  oscillators, we have the following: For each  $k = 1, \dots, N$ , there is a vector field  $X^{(k)}$  on  $\mathbb{T}^k$  such that if  $\varphi_t^{(k)}$  is the flow generated by  $X^{(k)}$ , then (i)  $\varphi_t^{(k)}$  describes the dynamics of the network defined by the first  $k$  oscillators and the relations among them, and (ii)  $\varphi_t^{(k+1)}$  is a *skew-product* over  $\varphi_t^{(k)}$ , that is, the vector field  $X^{(k+1)}$  on  $\mathbb{T}^{k+1}$  has the form

$$X^{(k+1)}(\theta_1, \dots, \theta_{k+1}) = (X^{(k)}(\theta_1, \dots, \theta_k), Y_{(\theta_1, \dots, \theta_k)}(\theta_{k+1})) \quad (5)$$

where  $\{Y_{(\theta_1, \dots, \theta_k)}\}$  is a family of vector fields on  $S^1$  parametrized by  $(\theta_1, \dots, \theta_k) \in \mathbb{T}^k$ . In particular,  $\varphi_t^{(N)} = \varphi_t$ . In the system defined by (5), we refer to  $\varphi_t^{(k)}$  on  $\mathbb{T}^k$  as the flow on the *base*, and each copy of  $S^1$  over  $\mathbb{T}^k$  as a *fiber*.

**Proposition 3.1.** *The flow of every acyclic network of  $N$  oscillators with no inputs can be represented by a hierarchy of skew-products with 1-dimensional fibers.*

**Proof:** Let  $\mathcal{N}_m$  be the set of oscillators  $j$  with  $m(j) = m$ . Assign an ordering to the oscillators so that all the oscillators in  $\mathcal{N}_0$  come first, followed by those in  $\mathcal{N}_1$ , then  $\mathcal{N}_2$ , and so on. The order within each  $\mathcal{N}_m$  is immaterial. Let us denote this ordering by  $i_1 < i_2 < \dots < i_N$ . A skew-product is built inductively as follows: For  $k \geq 1$ , consider the subnetwork consisting of oscillators  $i_1, \dots, i_k$ . None of the oscillators  $i_j, j \leq k$ , receives input from any of the oscillators  $i_\ell, \ell > k$ . (To see this, note that  $i_\ell \rightarrow i_j$  implies  $m(i_j) > m(i_\ell)$  by definition, but this is impossible under the ordering we have chosen.) Therefore, the dynamics of oscillators  $i_1, \dots, i_k$  as a subsystem of the entire network may be described by a vector field of the form  $X^{(k)}(\theta_{i_1}, \dots, \theta_{i_k})$ , obtained by projecting  $X^{(N)}$  onto these  $k$  coordinates. Starting with  $k = 1$ , the skew-products in the lemma are constructed inductively for increasing  $k$ .  $\square$

Next we generalize to acyclic networks with stimuli. Such networks can also be represented by a directed graph of the type described above, except that some of the nodes correspond to stimuli and others to oscillators. If  $i$  is a stimulus and  $j$  an oscillator, then  $i \rightarrow j$  if oscillator  $j$  receives information directly from stimulus  $i$ . No arrow can terminate at a stimulus, so that  $m(i) = 0$  if  $i$  is

a stimulus. Clearly, a network driven by stimuli is acyclic if and only if the corresponding network without stimuli is acyclic.

Proceeding to skew-product representations, consider first the case of a single oscillator driven by a single stimulus. Let  $\Omega$  denote the set of all Brownian paths defined on  $[0, \infty)$ , and let  $\sigma_t : \Omega \rightarrow \Omega$  be the time shift. Then the dynamics of the stochastic flow discussed in Sect. 2.1 can be represented as the skew-product on  $\Omega \times S^1$  with

$$\Phi_t : (\omega, x) \mapsto (\sigma_t(\omega), F_{0,t;\omega}(x)).$$

Similarly, a network of  $N$  oscillators driven by  $q$  independent stimuli can be represented as a skew-product with base  $\Omega^q$  (equipped with product measure) and fibers  $\mathbb{T}^N$ .

**Proposition 3.2.** *The dynamics of an acyclic network driven by  $q$  stimuli can be represented by a hierarchy of skew-products over  $\Omega^q$  with 1-dimensional fibers.*

The proof is identical to that of Proposition 3.1, except that when enumerating the nodes of the graph, we first list all of the stimuli (in any order) before listing the oscillators.

### 3.2 Lyapunov exponents of acyclic networks

Consider a network of  $N$  oscillators driven by  $q$  independent stimuli. We first review some notation. Let  $\omega \in \Omega^q$  denote a  $q$ -tuple of Brownian paths, and let  $F_{0,t;\omega}$  denote the corresponding stochastic flow on  $\mathbb{T}^N$ . For a fixed  $\omega \in \Omega^q$ ,  $x \in \mathbb{T}^N$  and tangent vector  $v$  at  $x$ , define the *Lyapunov exponent*

$$\lambda_\omega(x, v) = \lim_{t \rightarrow \infty} \frac{1}{t} \log |DF_{0,t;\omega}(x)v| \quad (6)$$

if this limit exists. If  $\mu$  is a stationary measure of the stochastic flow, then for a.e.  $\omega$  and  $\mu$ -a.e.  $x$ ,  $\lambda_\omega(x, v)$  is well defined for all  $v$ . The following is the main result of this section:

**Theorem 2.** *Consider a network of  $N$  oscillators driven by  $q$  independent stimuli, and let  $\mu$  be a stationary measure for the stochastic flow. Assume*

- (a) *the network is acyclic, and*
- (b)  *$\mu$  has a density on  $\mathbb{T}^N$ .*

*Then  $\lambda_\omega(x, v) \leq 0$  for a.e.  $\omega \in \Omega^q$  and  $\mu$ -a.e.  $x$ .*

One way to guarantee that condition (b) is satisfied is to set  $\varepsilon_i$  to a very small but strictly positive value if oscillator  $i$  is not originally thought of as receiving a stimulus, so that  $\varepsilon_i > 0$  for all  $i$ . Such tiny values of  $\varepsilon_i$  have minimal effect on the network dynamics. Condition (b) may also be satisfied in many cases where some  $\varepsilon_i = 0$  if suitable hypoellipticity conditions are satisfied, but we do not pursue this here [26].

Before proceeding to a proof, it is useful to recall the following facts about Lyapunov exponents. For a.e.  $\omega$  and  $\mu$ -a.e.  $x$ , there is an increasing sequence of subspaces  $\{0\} = V_0 \subset V_1 \subset \dots \subset V_r = \mathbb{R}^N$  and numbers  $\lambda_1 < \dots < \lambda_r$  such that  $\lambda_\omega(x, v) = \lambda_i$  for every  $v \in V_i \setminus V_{i-1}$ . The subspaces depend on  $\omega$  and  $x$ , but the exponents  $\lambda_j$  are constant a.e. if the flow is ergodic. We call

a collection of  $N$  vectors  $\{v_j\}$  a *Lyapunov basis* if exactly  $\dim(V_i) - \dim(V_{i-1})$  of these vectors are in  $V_i \setminus V_{i-1}$ . If  $\{v_j\}$  is a Lyapunov basis, then for any  $u, v \in \{v_j\}$ ,  $u \neq v$ ,

$$\lim_{t \rightarrow \infty} \frac{1}{t} \log |\sin \angle(DF_{0,t;\omega}(x)u, DF_{0,t;\omega}(x)v)| = 0, \quad (7)$$

that is, angles between vectors in a Lyapunov basis do not decrease exponentially fast; see *e.g.*, [43] for a more detailed exposition.

**Proof:** Since the network is acyclic, it factors into a hierarchy of skew-products. The  $k$ th of these is a stochastic flow  $F_{0,t;\omega}^{(k)}$  on  $\mathbb{T}^k$ . It describes the (driven) dynamics of the first  $k$  oscillators assuming they have been reordered so that oscillator  $i$  is upstream from or unrelated to oscillator  $j$  for  $i < j$ . Let  $\mu^{(k)}$  denote the projection of  $\mu$  onto  $\mathbb{T}^k$ . Then  $\mu^{(k)}$  is a stationary measure for  $F_{0,t;\omega}^{(k)}$ , and it has a density since  $\mu$  has a density. We will show inductively in  $k$  that the conclusion of Theorem 2 holds for  $F_{0,t;\omega}^{(k)}$ .

For  $k = 1$ ,  $\lambda_\omega(x, v) \leq 0$  for a.e.  $\omega$  and  $\mu^{(1)}$ -a.e.  $x$ . This is a consequence of Jensen's Inequality; see *e.g.*, [21], Sect. 2.2, for more detail.

Assume we have shown the conclusion of Theorem 2 up to  $k - 1$ , and view  $F_{0,t;\omega}^{(k)}$  as a skew-product over  $\Omega^q \times \mathbb{T}^{k-1}$  with  $S^1$ -fibers. Choose a vector  $v_k$  in the direction of the  $S^1$ -fiber. Note that this direction is invariant under the variational flow  $DF_{0,t;\omega}^{(k)}$  due to the skew-product structure. Starting with  $v_k$ , we complete a Lyapunov basis  $\{v_1, \dots, v_k\}$  at all typical points. Due to the invariance of the direction of  $v_k$ , we may once more use Jensen's Inequality to show that  $\lambda_\omega(x, v_k) \leq 0$  for a.e.  $x$  and  $\omega$ . We next consider  $v_i$  with  $i < k$ . First, define the projection  $\pi : \mathbb{T}^k \rightarrow \mathbb{T}^{k-1}$ , and note that

$$|DF_{0,t;\omega}^{(k)}(x)v_i| = \frac{|\pi(DF_{0,t;\omega}^{(k)}(x)v_i)|}{|\sin \angle(v_k, DF_{0,t;\omega}^{(k)}(x)v_i)|}.$$

Due to Eq. (7), we have  $\lambda_\omega(x, v_i) = \lim_{t \rightarrow \infty} \frac{1}{t} \log |\pi(DF_{0,t;\omega}^{(k)}(x)v_i)|$ . But the skew-product structure yields  $\pi(DF_{0,t;\omega}^{(k)}(x)v_i) = DF_{0,t;\omega}^{(k-1)}(\pi x)(\pi v_i)$ , so by our induction hypothesis,  $\lambda_\omega(x, v_i) \leq 0$ .  $\square$

**Remarks on reliability of acyclic networks:** Our conclusion of  $\lambda_{\max} \leq 0$  falls short of reliability, which corresponds to  $\lambda_{\max} < 0$ . When there are free-rotating oscillators in a network, *i.e.* oscillators that are not driven by either a stimulus or another oscillator, then clearly  $\lambda_{\max} = 0$ . When no free-rotating oscillators are present, typically one would expect  $\lambda_{\max} < 0$ . We do not have a rigorous proof, but this intuition is supported by numerical simulations.

Arguments similar to those in the proof of Theorem 2 (but in the absence of stimuli and without the use of an invariant measure) give the following:

**Proposition 3.3.** *Acyclic networks are never intrinsically chaotic, in the sense that at Lebesgue-a.e.  $x \in \mathbb{T}^N$ , all Lyapunov exponents (with  $\limsup$  instead of limit in Eq. (6)) are  $\leq 0$ .*

### 3.3 Modular decompositions and quotient systems

We next describe how the reliability of more general networks may be analyzed by decomposition into subunits. Consider a graph with nodes  $\{1, \dots, N\}$  as in the beginning of Sect. 3.1, and let  $\sim$  be an equivalence relation on the set  $\{1, \dots, N\}$ . The quotient graph defined by  $\sim$  has as its nodes the equivalence classes  $[i]$  of  $\sim$ , and we write  $[i] \rightarrow [j]$  if there exists  $i' \in [i]$  and  $j' \in [j]$  such that  $i' \rightarrow j'$ . The following is a straightforward generalization of Proposition 3.2:

**Proposition 3.4.** *In a network of oscillators driven by  $q$  independent stimuli, if an equivalence relation leads to an acyclic quotient graph, then the dynamics of the network can be represented by a hierarchy of skew-products over  $\Omega^q$ , with the dimensions of the fibers equal to the sizes of the corresponding equivalence classes.*

We pause to discuss in more detail the structure in Prop 3.4, as it is important in the rest of this paper. An equivalence relation on the nodes of a network describes a decomposition of the network into smaller subunits called *modules*. Introducing directed edges between modules as above, we obtain what we call a *quotient network* in this paper. Assume this quotient network is acyclic, and let  $M_1, M_2, \dots, M_p$  be the names of the modules ordered in such a way that  $M_i$  is upstream from or unrelated to  $M_j$  for all  $j > i$ . Let  $k_j$  be the number of nodes in module  $M_j$ . For  $s_i = k_1 + k_2 + \dots + k_i$ , let  $F_{0,t,\omega}^{(s_i)}$  denote, as before, the stochastic flow describing the dynamics within the union of the first  $i$  modules; we do not consider  $F_{0,t,\omega}^{(s)}$  when  $s \neq s_i$  for some  $i$ . The dynamics of the entire network can then be built up layer by layer as follows: We begin with the stochastic flow  $F_{0,t,\omega}^{(k_1)}$ . Then proceed to  $F_{0,t,\omega}^{(k_1+k_2)}$ , which we view as a skew-product over  $F_{0,t,\omega}^{(k_1)}$ . This is followed by  $F_{0,t,\omega}^{(k_1+k_2+k_3)}$ , which we view as a skew-product over  $F_{0,t,\omega}^{(k_1+k_2)}$ , and so on.

Let  $\lambda_1^{(1)}, \dots, \lambda_{k_1}^{(1)}$  denote the Lyapunov exponents of  $F_{0,t,\omega}^{(k_1)}$ . Clearly, these are the Lyapunov exponents of a network that consists solely of module  $M_1$  and the stimuli that feed into it. We wish, however, to view  $M_1$  as part of the larger network. If  $\lambda_{\max}^{(1)} \equiv \max_j \lambda_j^{(1)} > 0$ , we say *unreliability is produced within  $M_1$* . An interesting question is the effect of this unreliability on sites downstream. Leaving this to Sect. 4, we continue with the present discussion: For  $i > 1$ , let  $\lambda_1^{(i)}, \dots, \lambda_{k_i}^{(i)}$  denote the *fiber Lyapunov exponents* in the skew-product representation of  $F_{0,t,\omega}^{(s_i)}$  over  $F_{0,t,\omega}^{(s_{i-1})}$ , and let  $\lambda_{\max}^{(i)} = \max_j \lambda_j^{(i)}$ . Then  $\lambda_{\max}^{(i)} > 0$  has the interpretation that *unreliability is produced within module  $M_i$  as it operates in the larger network*. It is important not to confuse this with the Lyapunov exponents of module  $M_i$  in isolation, an issue we will follow up in Sect. 6.

Analogous interpretations for the zero-input systems are obvious: for  $i > 1$ ,  $\lambda_{\max}^{(i)} > 0$  at  $\varepsilon = 0$  means there is intrinsic network chaos within the module  $M_i$  as a subsystem of the larger system, and so on.

The proof of the following result is virtually identical to that of Theorem 2:

**Proposition 3.5.** *Suppose for a driven network there is an equivalence relation leading to an acyclic quotient graph. Then, with respect to any ergodic stationary measure  $\mu$ , the numbers  $\lambda_j^{(i)}, 1 \leq i \leq p, 1 \leq j \leq k_i$ , are precisely the Lyapunov exponents of the network.*

Proposition 3.5 says in particular that if, in each of the  $p$  skew-products in the hierarchy, the fiber Lyapunov exponents are  $\leq 0$ , i.e., if no unreliability is produced within any of the modules, then

$\lambda_{\max}$  for the entire network is  $\leq 0$ . Conversely, if unreliability is produced within any one of the modules as it operates within this network, then  $\lambda_{\max} > 0$  for the entire network. On the practical level, the skew product structure (which implies that  $DF_{0,t;\omega}$  is block-lower-triangular) and the Proposition together give a more efficient way to numerically compute Lyapunov exponents of networks with acyclic quotients.

**Important remarks.** *In the rest of this paper, we will often take the view that the network in question is equipped with a modular decomposition connected by an acyclic graph.* Such a decomposition always exists for any network, but it can be trivial (e.g., when the entire network is a single module). If the decomposition is nontrivial and  $\lambda_{\max} > 0$  for the network, Proposition 3.5 enables us to localize the *source* of the unreliability, i.e., to determine in which module unreliability is produced via their fiber Lyapunov exponents. In particular, modules that are themselves acyclic cannot produce unreliability.

As noted earlier, the idea of “upstream”–“downstream” for acyclic networks extends to modules connected by acyclic graphs, so that it makes sense to speak of a module as being downstream from another module, or a site as being downstream from another site, meaning the modules in which they reside are so related.

## 4 Propagation of unreliability

In this section, we address the following basic question: *Under what conditions will unreliability generated in one part of a network propagate downstream?* In Sect. 4.1, we discuss how to measure unreliability at specific network sites, and in Sect. 4.2, we address the question posed.

### 4.1 Measuring reliability at individual network sites

Often, it is the response of a network measured at specific oscillators (or *sites*) that is of relevance, rather than the response of the network as a whole. While  $\lambda_{\max} > 0$  tells us that there is unreliability somewhere in the system, it does not tell us which oscillators are affected. To capture the idea of reliability at individual sites, recall that the reliability of the entire system is reflected in the sample measures  $\mu_\omega$  (see Sect. 1.2). By the same reasoning, the reliability at site  $i$  is reflected in the marginals of  $\mu_\omega$  in the variable  $\theta_i$ ; we denote this marginal distribution by  $\mu_{\omega,i}$ . We say a network is *reliable at site  $i$*  if  $\mu_{\omega,i}$  is concentrated at a single point; the more uniformly distributed these projected sample measures are, the greater the *site unreliability*. These ideas are easily generalized to groups of more than one site, but we will treat only single site reliability.

The following are three standard ways in which the distribution of  $\mu_{\omega,i}$  can be described:

A. *Site entropy.* For each  $i$  and  $\omega$ , we let  $H(i, \omega)$  denote the entropy of the distribution  $\mu_{\omega,i}$ , i.e., if  $\rho_{\omega,i}$  is the density of  $\mu_{\omega,i}$  with respect to Lebesgue measure on  $S^1$ , then

$$H(i, \omega) = - \int_{S^1} \log \rho_{\omega,i} d\rho_{\omega,i} ,$$

and we set  $H(i, \omega) = -\infty$  if  $\mu_{\omega, i}$  is singular. The *site entropy*  $H(i)$  is defined to be the expected value of this random variable, *i.e.*,  $H(i) = \int H(i, \omega) P(d\omega)$ . In practice,  $H(i)$  is computed as  $\lim_{T \rightarrow \infty} \frac{1}{T} \int_0^T H(i, \sigma_t(\omega)) dt$  via the Ergodic Theorem. This number can range from  $-\infty$  to 0, with  $H(i) = 0$  corresponding to uniform distribution and  $H(i) = -\infty$  corresponding to the distribution being singular with respect to Lebesgue measure. A drawback of site entropy is that it does not distinguish among singular distributions.

*B. Information dimension.* We define

$$D(i, \omega) = \lim_{k \rightarrow \infty} D_k(i, \omega) \quad \text{where} \quad D_k(i, \omega) = \frac{-\sum_{j=1}^k p_j \log p_j}{\log k}.$$

In the quantity on the right,  $S^1$  is divided into  $k$  equal intervals, and  $p_j$  is the probability with respect to  $\mu_{\omega, i}$  of finding the phase of oscillator  $i$  in the  $j^{\text{th}}$  subinterval. The relevant quantity is then  $D(i) = \int D(i, \omega) P(d\omega)$ . This takes values on  $[0, 1]$ , with  $D(i) = 1$  corresponding to any distribution having a density. Information dimension does not, for example, distinguish between the uniform distribution on  $S^1$  and a distribution supported uniformly on a tiny subinterval of  $S^1$ .

*C. Cumulative distribution functions (CDFs).* The most direct way to assess site distributions is to compute the CDF of  $\mu_{\omega, i}$ . This is numerically very simple to do, and is especially effective in establishing whether the measure is concentrated at a single point. A drawback of using CDFs is that it is not a number. Moreover, to be certain that one is seeing “typical” CDFs, one needs to compute them for  $\mu_{\omega, i}$  for many values of  $\omega$ , as CDFs cannot be averaged.

Above, we discussed various ways to assess  $\mu_{\omega, i}$  from a purely theoretical standpoint. Returning to the situation at hand, recall from Theorem 1 that when  $\lambda_{\max} > 0$ , *i.e.* when the system is unreliable,  $\mu_{\omega}$  is a random SRB measure. These measures have densities on complicated families of smooth manifolds. In particular, they have dimensions  $> 1$ ; *e.g.* in the case of 2 oscillators, the dimension of the random SRB measures is  $1 + \alpha$  for some  $\alpha \in (0, 1)$  where  $\alpha$  describes the dimension of the fractal part. A well known result in analysis [24] tells us that when measures of dimensions  $> 1$  are projected onto 1-dimensional subspaces, the projected measures have a density for projections along *almost all* directions. Now not all projections are “good” in this sense, and we cannot be certain that the projection onto any particular site is “good” (projections onto sites upstream from where unreliability is produced are obviously not). Still, *if* the projection to site  $i$  is good, then  $\lambda_{\max} > 0$  would imply that  $\mu_{\omega, i}$  has a density. This being the case, it is more important to be able to compare different distributions with densities than to distinguish different singular distributions. We therefore favor site entropy over information dimension as a measure of site reliability.

In this paper, we will use a combination of site entropy and CDFs: If the computed values of  $H(i)$  appear bounded below, then it is safe to conclude site unreliability, and the closer  $H(i)$  is to 0, the more unreliable. If, on the other hand, the computed values of  $H(i)$  appear unbounded, then CDFs are used to confirm site reliability.

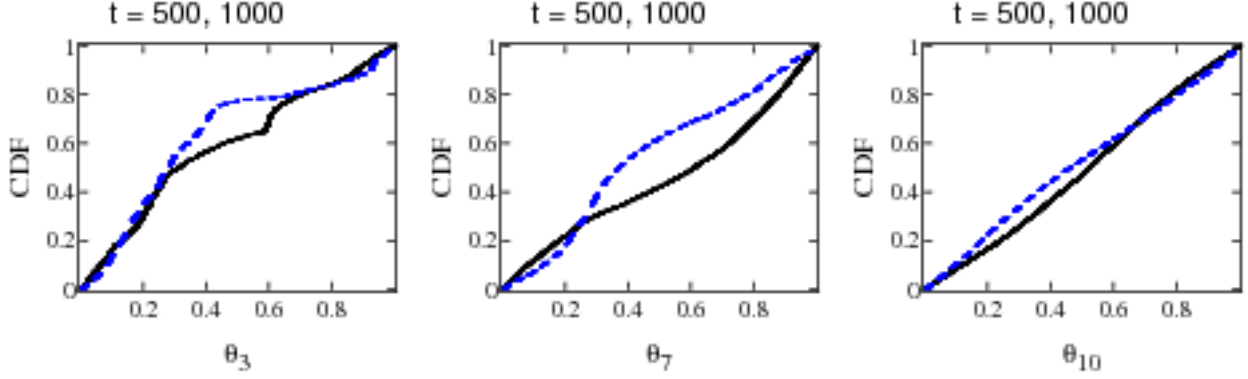
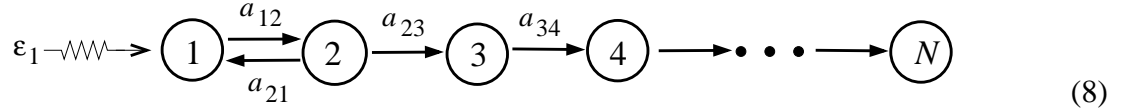


Figure 3: Site distributions for the system (8) with  $N = 10$ . Shown are the site- $i$  CDFs for  $i = 3, 7, 10$ , at times  $t = 500$  (solid) and  $t = 1000$  (dash). The parameters are as follows: for the (1,2) subsystem, we set  $\omega_1 = 1$ ,  $\omega_2 = 1.05$ ,  $a_{12} = 1$ ,  $a_{21} = 1.18$ , and  $\varepsilon = 1$  (so that  $\lambda_{\max} \approx 0.13$ ). For  $i \geq 3$ , we draw  $\omega_i$  from  $[0.9, 1.1]$  and  $a_{i,i+1}$  from  $\pm[0.6, 1.2]$ .

## 4.2 Sites downstream from unreliable modules

We now return to the question of propagation of unreliability to sites downstream from an unreliable module. The simplest network with which to investigate this is the  $N$ -chain system



Suppose we choose  $a_{12}$ ,  $a_{21}$ , and  $\varepsilon_1$  so that the (1,2)-subsystem is unreliable. Notice that no unreliability is produced elsewhere. The question is: will this unreliability be observable downstream, at sites  $i = 3, 4, \dots, N$ , or does it somehow “dissipate?” We run the following numerical experiment: we set  $\omega_1 = 1$ ,  $\omega_2 = 1.05$ ,  $a_{12} = 1$ ,  $a_{21} = 1.05$ , and  $\varepsilon_1 = 1$ , so that the Lyapunov exponent  $\lambda_{\max}$  of the (1,2)-subsystem is  $\approx 0.1$ . For  $i \geq 3$ , we draw randomly (and fix)  $\omega_i$  from  $[0.9, 1.1]$  and  $a_{i,i+1}$  from  $\pm[0.6, 1.2]$ . Computing the site entropies<sup>3</sup>  $H(i)$  for sites  $i = 3, 7, 10$ , we find:

Site	$i = 3$	$i = 7$	$i = 10$
Entropy $H(i)$	-0.4	-0.2	-0.01

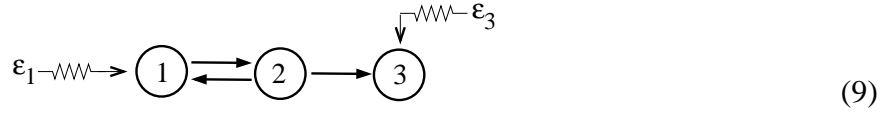
To help interpret these numbers, recall that identifying  $S^1$  with  $[0, 1]$ , the entropy of the uniform distribution on an interval  $[a, b]$  is  $\log(b - a)$ , and  $\log \frac{1}{2} \approx -0.7$ . The data above thus indicate that the site distributions are fairly uniform, and in fact seem to become more uniform for sites farther downstream. Fig. 3 shows the corresponding CDFs for some sites at representative times; CDFs at other sites are qualitatively similar. The graphs clearly show that unreliability propagates.

We give two explanations for why one should expect this result of propagating site unreliability. The first is a plausibility argument along the lines of the projection argument in Sect. 4.1: it is possible – but highly unlikely – that the SRB measure  $\mu_\omega$  would project to point masses in any

<sup>3</sup>We compute site entropies by simulating the response of 10,000 initial conditions to the same realization of the stimulus, then applying the “binless” estimator of Kozachenko and Leonenko [18] (see also [38]).

of the 8 directions corresponding to the 8 sites downstream. A second, perhaps more intuitive explanation, is as follows. Consider site 3 in the system (8). Fix a realization of the stimulus, and let  $(\theta_1, \theta_2, \theta_3)$  denote the 3 phase coordinates. For each choice of  $(\theta_1(0), \theta_2(0))$ , the third oscillator receives a sequence of coupling impulses from the (1,2)-subsystem. Since the (1,2)-subsystem is unreliable, different choices of  $\theta_1(0)$  and  $\theta_2(0)$  will produce different sequences of coupling impulses to oscillator 3, in turn leading to different values of  $\theta_3(t)$ . This is synonymous with site unreliability for oscillator 3.

What happens if an oscillator receives inputs from more than one source with competing effects? The simplest situation is an oscillator driven by both an unreliable module upstream and an input stimulus, as depicted in Diagram (9). Note the presence of competing terms: As we have just seen, the unreliable module leads to unreliability at site 3. However, the stimulus  $\varepsilon_3$  has a stabilizing effect on that oscillator.



In the results tabulated below, the parameters used are  $\omega_1 = 1$ ,  $\omega_2 = 1.05$ ,  $a_{12} = 1$ ,  $a_{21} = 1.15$ , and  $\varepsilon_1 = 1$  (so that the (1,2)-subsystem is again unreliable),  $a_{23} = 0.5$  and  $\omega_3 = 0.93$ . The site entropy  $H(3)$  is computed for various values of  $\varepsilon_3$ . We find:

Stimulus amplitude	$\varepsilon_3 = 0.2$	$\varepsilon_3 = 1$	$\varepsilon_3 = 2$
Site entropy $H(3)$	-0.4	-1.2	-2

These numbers tell us that at  $\varepsilon_3 = 0.2$ , the distribution at site 3 is fairly uniform, and that this distribution becomes more concentrated as  $\varepsilon_3$  increases. The CDFs (not shown) confirm this. When  $\varepsilon_3 = 2$ , for example, about 80% of the distribution  $\mu_{\omega,3}$  is concentrated on an interval of length  $\leq 1/5$  roughly 70% of the time. These data show that the source of reliability, *i.e.*, the stimulus into oscillator 3, attenuates the propagation of unreliability; we call this phenomenon *interference*. Moreover, we find that when  $\varepsilon_3$  is increased further, the support of a large fraction of  $\mu_{\omega,3}$  shrinks to smaller and smaller intervals, decreasing the entropy and reflecting a greater tendency to form random sinks in oscillator 3. However, simulations also show that oscillator 3 does not become fully site reliable even at fairly strong forcing. This is also expected: intuitive arguments similar to those above suggest that once created, site unreliability cannot be completely destroyed at downstream sites. To summarize:

**Observation 3:** *Unreliability, once generated, propagates to all sites downstream.*

We finish by clarifying the relation between the material in Sect. 3.3 and this section:

**Propagation versus production of unreliability:** The topic of Sect. 4 is whether or not unreliability created upstream propagates, *i.e.*, whether it can be observed downstream. This concept complements an idea introduced in Sect. 3.3, namely the production of *new* unreliability within a module as measured by the positivity of fiber Lyapunov exponents. Mathematically, site reliability (or unreliability) is reflected in the marginals of  $\mu_{\omega}$  at the site in question, while the unreliability

produced within a module is reflected in the dynamics and conditional measures of  $\mu_\omega$  on fibers. Naturally, when a module produces unreliability in the sense of Sect. 3.3, its sites will also show unreliability in the sense of Sect. 4.1, and one cannot separate what is newly produced from what is passed down from upstream.

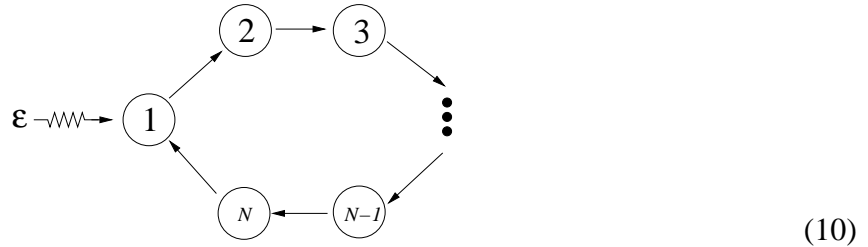
## 5 Examples: reliability and unreliability in small networks

In [21], we carried out a detailed study of a coupled oscillator pair. One may seek a similar understanding of other small networks, but any classification grows rapidly in complexity with the number of sites. In this section, we do not attempt a systematic study, but provide a few examples of small networks exhibiting various behaviors.

In all the examples in this section,  $\omega_i \in [0.95, 1.05]$ .

### 5.1 The $N$ -ring

Our first class of examples is a direct generalization of the 2-loop studied in [21], namely networks of “ring” type:



The main point of this example is to demonstrate that the system above exhibits both reliable and unreliable dynamics. Along the way, we also briefly illustrate two interesting phenomena about which we have little explanation.

**Example 1** (*Amplification effects along loop?*) For  $N = 2, 3, \dots, 7$ , we fix  $a_{i,i+1}$  for  $i = 1, \dots, N - 1$ , and let  $a_{N,1}$  vary. Our findings can be summarized as follows:

- (a) With all the  $a_{i,i+1} \approx 1$ , the system is *reliable* for  $a_{N,1} \in [0, 2]$  and  $\varepsilon < 2$ .
- (b) For  $\varepsilon = 1$  and  $a_{i,i+1} \sim \frac{1}{N}$  suitably chosen, the system is *unreliable* for  $a_{N,1} \in [0.6, 2]$ .

Results of numerical simulations for  $N = 7$  are shown in Fig. 4. For case (a) we randomly choose  $\omega_j$  and  $a_{i,i+1} \in [0.95, 1.05]$  for  $1 \leq j \leq N$  and  $1 \leq i < N$ . For case (b), we start the same way, but multiply all the  $a_{i,i+1}$  chosen by a constant  $c$ . As we tune  $c$  from 1 down to 0, we find that in each case, pictures similar to that in Fig. 4(b) are produced for a range of  $c \sim \frac{1}{N-1}$  where  $N$  is the size of the ring. Simulations were repeated for different choices of  $\omega_j$  and  $\tilde{a}_{i,i+1}$ , to similar effect. The exact  $c$ 's that produce the most unreliable behaviors, however, vary with the choices of  $\omega_j$  and  $a_{i,i+1}$ ;  $\frac{1}{N-1}$  is only a rough approximation.

Details aside, the following trend as  $N$  increases from 2 to 7 is unmistakable: Given that we use roughly equal  $a_{i,i+1}$  for  $1 \leq i < N$  and set  $a_{N,1} \approx 1$ , the values of  $a_{i,i+1}$  for which unreliable dynamics occur decrease steadily as  $N$  increases. It is as though coupling effects are amplified

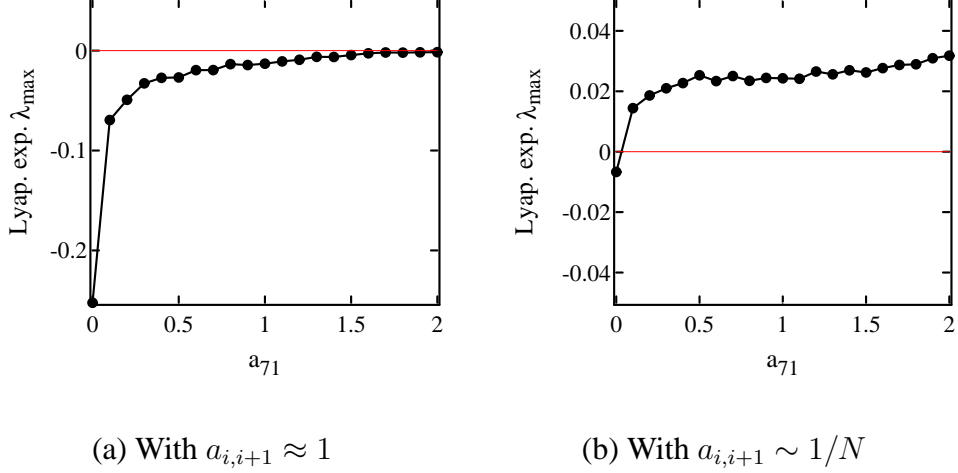


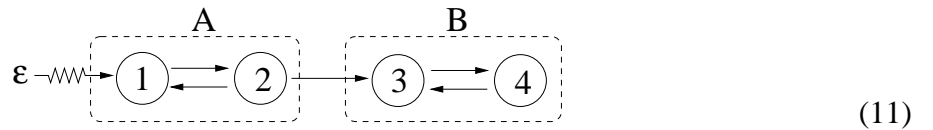
Figure 4: Amplification effect in  $N$ -ring, with  $N = 7$ . We show the Lyapunov exponent  $\lambda_{\max}$  as a function of  $a_{N,1}$ . In (a), the coupling constants  $a_{i,i+1}$  for  $i = 1, 2, \dots, N - 1$  are all  $\approx 1$ . In (b), they are  $\sim 1/N$  (see text). In both plots,  $\varepsilon = 1$ .

along the loop, giving rise to an effective coupling “ $a_{1,N}$ ”  $\sim 1$ . (For  $N = 2$ , the system is known to be most unreliable when  $a_{12}$  and  $a_{21}$  are roughly comparable; see [21].) Whatever the explanation, this  $N$ -ring example promises to be interesting (but we do not pursue it further here).

**Example 2** (*Cancellation effect by couplings of opposite signs?*) Given the conjectured amplification effect just described, it is natural to ask whether negative coupling terms along the loop would diminish the effects of positive coupling, and *vice versa*. This idea is validated in simulations. For example, for the 4-ring we find (as asserted above) that  $\lambda_{\max} < 0$  when the coupling constants are all  $\approx 1$ ; the plot is qualitatively similar to Fig. 4(a). However, if we flip the sign of any one of the 4 couplings to a value of  $\approx -1$  while leaving the rest at  $\approx 1$ , we then obtain  $\lambda_{\max} > 0$  and plots qualitatively similar to Fig. 4(b).

## 5.2 2-loops driving 2-loops

Here we study a new situation, in which one unreliable module drives another. Consider the system



We think of this network as consisting of two modules: the (1,2)-subsystem as Module A and the (3,4)-subsystem as Module B. From [21], we have a great deal of information about these 2-oscillator systems individually. Here, we investigate the unreliability produced within Module B when driven by Module A. Representing system (11) as a skew product with 2-dimensional fibers over a 2-dimensional base (as in Sect. 3.3), we let  $\lambda_{\max}^{fib}$  denote the largest fiber Lyapunov exponent for Module B.

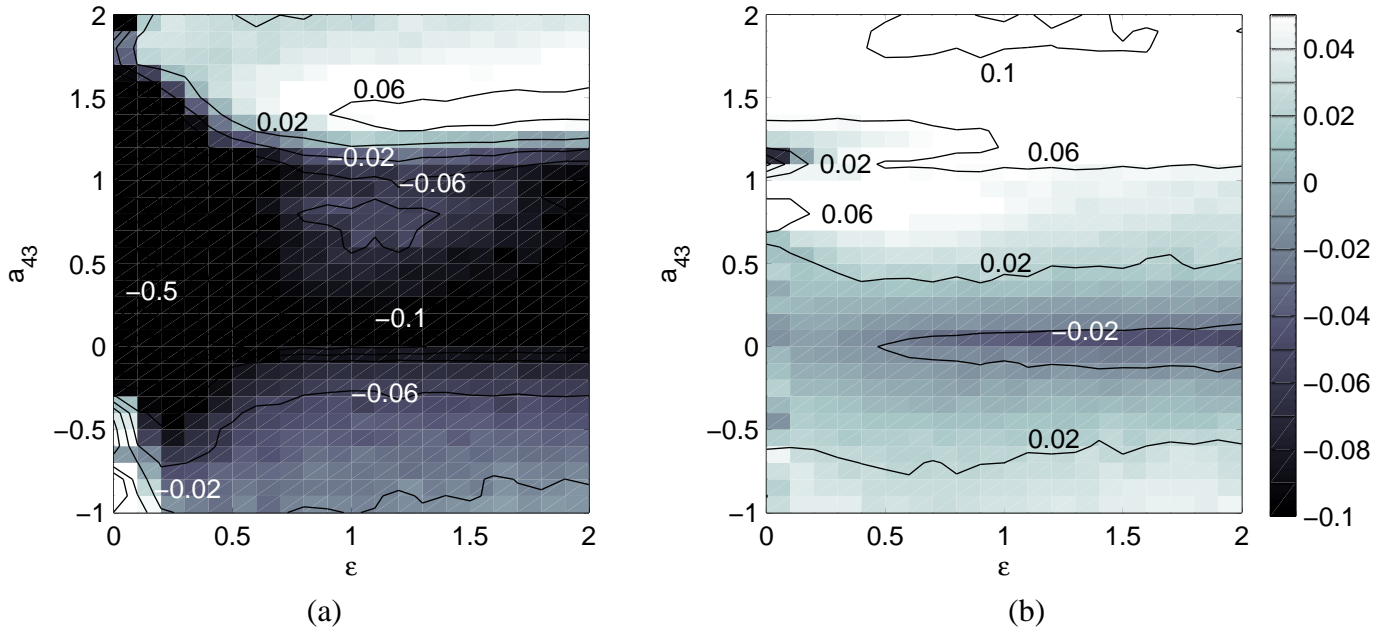


Figure 5: The maximum fiber exponent  $\lambda_{\max}^{fib}$  for Module B in system (11), as a function of  $\varepsilon$  and  $a_{43}$ . In (a), the parameters are  $a_{12} = 1.1$ ,  $a_{21} = 0.8$ ,  $a_{23} = 0.5$ , and  $a_{34} = 1$ . In (b), the parameters are  $a_{12} = -1.1$ ,  $a_{21} = -1.2$ ,  $a_{23} = 0.95$ , and  $a_{34} = 1$ . In both cases, we use  $\omega_1 = 1.03$ ,  $\omega_2 = 0.98$ ,  $\omega_3 = 1$ , and  $\omega_4 = 1.1$ . **Remark on plots:** We have chosen the dynamic range in shading the figures to allow meaningful comparison of figures; a side effect is that some contour lines may not be visible. We always indicate the actual range of values through explicit labels.

We fix two sets of parameters for which Module A is known to be unreliable. For one set, Module A has mutually “excitatory” coupling, with  $a_{12}, a_{21} > 0$ ; for the other, Module A has mutually inhibitory coupling, with  $a_{12}, a_{21} < 0$ . We then perform numerical experiments (see Fig. 5) in which we fix  $a_{34} = 1$  and vary  $a_{43}$  and the system input amplitude  $\varepsilon$ . Our findings are:

- (i) For both choices of parameters for Module A, unreliability is sometimes produced within Module B and sometimes not, depending on  $a_{43}$ .
- (ii) For most values of  $a_{34}, a_{43}$  and  $\varepsilon$ , Module B produces more unreliability (*i.e.*,  $\lambda_{\max}^{fib}$  is larger) when the oscillators in Module A are mutually inhibitory rather than excitatory.

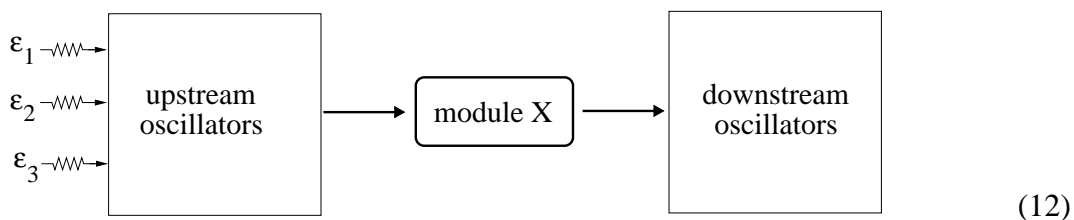
Both phenomena appear to be robust. We do not have an explanation for (ii), and will revisit (i) in Sect. 6.

The situation at  $\varepsilon = 0$  is shown in the leftmost column of each of the two panels in Fig. 5. As with the 3-ring in Sect. 2.2,  $\lambda_{\max}^{fib}$  at  $\varepsilon = 0$  varies sensitively with parameter. The production of intrinsic network chaos within Module B is evident for some parameters in both cases. For some parameter settings, this chaos is suppressed; see the bottom left panel. Overall, notice the strong influence of the  $\varepsilon = 0$  dynamics of Module B on its tendency to produce unreliability when the external stimulus is turned on.

## 6 Modules in isolation versus as part of larger system

Now that we have discussed both propagation of unreliability between modules and generation of unreliability within modules, we return to the strategy suggested in Sect. 3.3: to study the reliability of networks by analyzing their component modules separately. An obvious benefit of this strategy is that smaller modules are easier to test. However, the strategy will only be successful if the reliability of modules in isolation gives a good indication of their reliability when they are embedded in larger systems.<sup>4</sup>

Pictorially, the problem we face can be represented as follows:



Suppose our network can be decomposed into three parts: Module X, which is our module of interest, a (possibly large) component upstream from Module X, and a (possibly large) component downstream from Module X. The question is: *Can the reliability properties of Module X as a subsystem of this larger network be predicted by its reliability properties in isolation?*

First we need to clarify what we mean by the “reliability of a module in isolation”. We refer here to the reliability of the module (without the rest of the network) receiving stimuli with a simple, generic statistical structure; in this paper, this statistical structure is taken to be white noise. To simulate the correct phase-space geometry, it is important that the white noise be injected in a way that mimics network conditions. For example, if oscillators 1, 2, and 4 within Module X receive input from the rest of the network, then in analyzing the reliability properties of Module X in isolation, we must provide stimuli to the corresponding oscillators.<sup>5</sup> One should also use comparable forcing amplitudes, although it is less clear what exactly that means.

At the heart of this question is the following issue: A module embedded in a network may receive input from oscillators upstream in the form of coupling impulses; it may also hear directly from the external stimuli. Inputs from other oscillators resemble a point process of impulses with statistics somewhere between Poisson and periodic; moreover, when an oscillator receives kicks from multiple sources, these kicks may be correlated to varying degrees. The question is then whether reliability properties of a module are sufficiently similar under these different classes of inputs that they can be predicted from studies using white noise stimuli.

<sup>4</sup>This type of issue arises often in coupled nonlinear systems; it is very important yet seldom understood.

<sup>5</sup>To illustrate this point, consider a 2-oscillator system with unequal feedback/feedforward couplings: providing a stimulus to oscillator 1 leads to horizontal perturbations in  $(\theta_1, \theta_2)$ -space, whereas stimulating oscillator 2 leads to vertical perturbations. These two types of perturbations have different relations to the geometry of the intrinsic dynamics and can have different effects.

Let us return now to the situation depicted in the diagram above. For a quantitative study, we first compute  $\lambda_{\max}$  for Module X in isolation, subjected to white noise in a suitable range of amplitudes. These numbers will be compared to  $\lambda_{\max}^{fib}$  defined as follows: Consider the skew product in which the dynamics of the oscillators upstream from Module X are represented in the base and the dynamics within Module X are represented on the fibers. (The oscillators downstream from Module X are irrelevant.) The number  $\lambda_{\max}^{fib}$  is the largest fiber Lyapunov exponent (see Sect. 3.3). The following abbreviated language will be used in the remainder of this paper: when we speak of *the unreliability produced by a module*, we refer to the unreliability produced within that module when it operates as a subsystem in the larger network. The same abbreviation applies to intrinsic network chaos in a module.

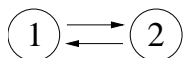
**Proposal:** *Whether unreliability is produced within Module X, i.e. whether  $\lambda_{\max}^{fib} > 0$  when  $\varepsilon > 0$ , is strongly influenced by*

- (a) *the reliability properties of Module X in isolation, and*
- (b) *the intrinsic dynamics within Module X when embedded in the full network, i.e.,  $\lambda_{\max}^{fib}$  at  $\varepsilon = 0$*

*Part (b) is especially relevant at small  $\varepsilon$ .*

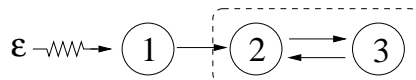
The proposal above is intended to give only a rough indication of the hills and valleys of the reliability profile of the module in question; no quantitative predictions are suggested. Part (b) of the proposal is largely a statement of continuity: when subjected to weak external stimuli, intrinsic network properties come through as expected. The rationale for (a) is that we have seen in a number of situations in general dynamical systems theory that the response of a system to external forcing depends considerably more strongly on its underlying geometry than on the type of forcing, especially when there are elements of randomness in the forcing, *e.g.* Poisson kicks and white-noise forcing have qualitatively similar effects (though purely periodic forcing can do peculiar things). A systematic study comparing different types of forcing is carried out in [22].

To support our proposal, we present below the results of a study in which the 2-cell system studied in [21], *i.e.*,

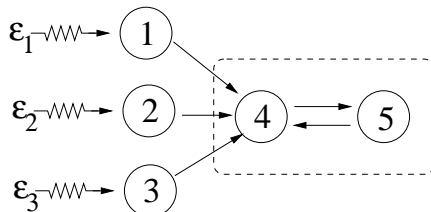


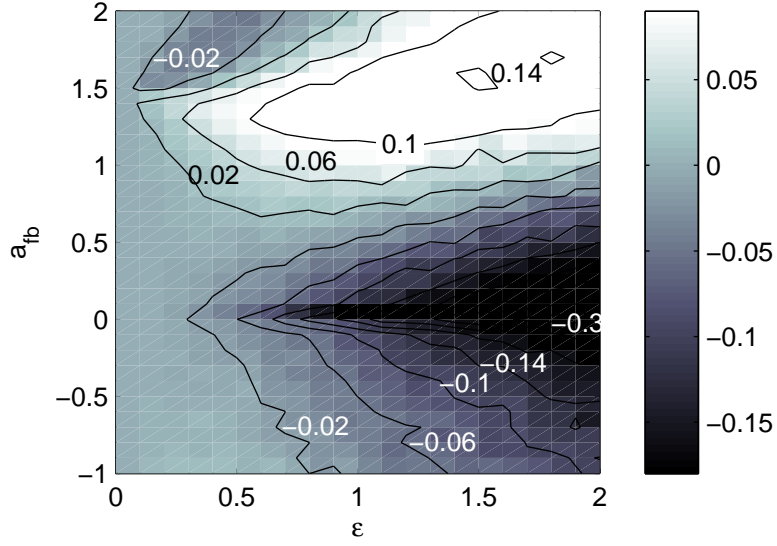
is used as the embedded module, that is, as Module X in the framework above. The three networks used in this study, with Module X enclosed in a dotted line, are:

Network A:

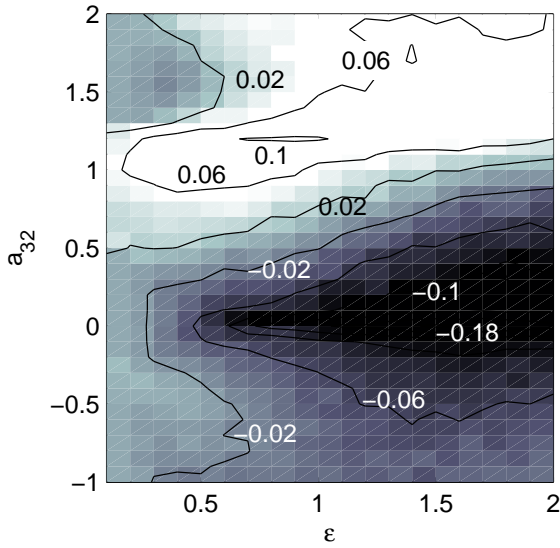


Network B:

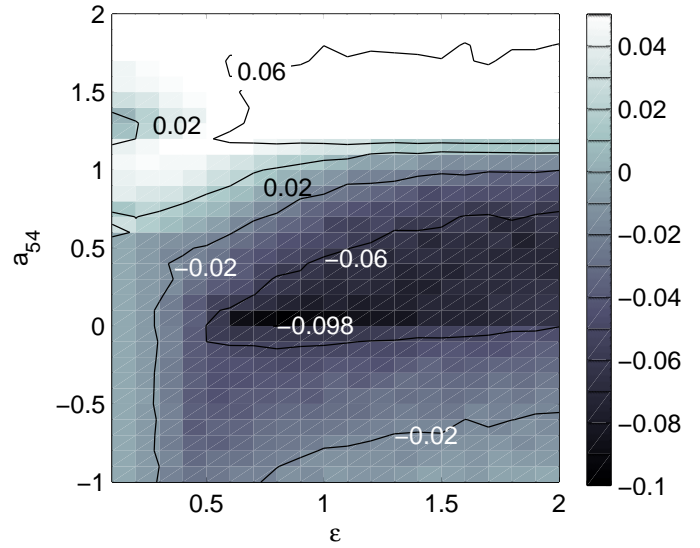




(a) Two oscillators in isolation



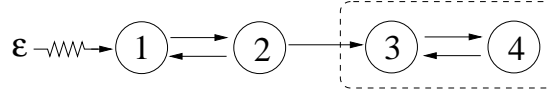
(b) Network A



(c) Network B

Figure 6: Reliability of Module X in isolation and as an embedded subsystem. In (a), we show  $\lambda_{\max}$  for Module X in isolation. The parameters are  $\omega_1 = 1$ ,  $\omega_2 = 1.1$ , and  $a_{\text{ff}} = 1$ . The corresponding modules in Networks A and B are given the same parameters. The other parameters are as follows: for Network A, we use  $\omega_1 = 0.97$ ,  $a_{12} = 0.7$ . For Network B, we draw  $\omega_i \in [0.95, 1.05]$  and set  $a_{i,4} = \frac{1}{3} \cdot (0.6, 0.8, 0.9)$  and  $\varepsilon_1 = \varepsilon_2 = \varepsilon_3 = \varepsilon$ .

Network C:



In Networks A and B, the oscillators that feed into Module X are themselves reliable. Network C is the system described in Sect. 5.2; as described there, parameters are chosen so that the subsystem (1,2) is unreliable. In each case, the feedforward coupling within Module X is set equal to 1, and the largest fiber exponent is computed as a function of the feedback coupling and  $\varepsilon$ . Sample plots for Networks A and B are shown in Fig. 6. For comparison, we have also included the plot for the 2-oscillator system in isolation (Fig. 12 in [21]), *i.e.* receiving a white noise input of strength  $\varepsilon$  at oscillator 1, to mimic the configuration in Networks A-C. Plots for Network C are in Fig. 5.

The resemblance of Figs. 6(b) and (c) to Fig. 6(a) is quite striking given the rather different inputs received by the Module X in isolation *vs.* embedded in Network B. This is evidence in favor of part (a) of the proposal above. Network C also gives qualitatively similar reliability profiles, although overall it is considerably more reliable for one set of parameters governing oscillators (1,2) than the other: see Figs. 5(a) and (b). As suggested by the second part of the proposal, there is a strong correlation between all of these overall tendencies and network dynamics at  $\varepsilon = 0$ , sensitive as the latter may be.

Here as in many other simulations not shown, we have found that even though the reliable and unreliable regions may shift and the magnitudes of  $\lambda_{\max}^{fib}$  may vary, the general tendency is that the reliability of Module X continues to resemble its reliability in isolation, that is, when it receives white noise inputs. We take these results to be limited confirmation of our proposal. In sum:

**Observation 4:** *The reliability profile of the two-oscillator system in isolation found in [21] is a reasonable guide to its reliability properties as a module embedded in a larger network.*

It remains to be seen whether this holds for other modules.

## 7 An illustrative example

We finish with the following example, which illustrates many of the points discussed in this paper.

The network depicted in Fig. 7(a) is made up of 9 oscillators. It receives a single input stimulus through oscillator 1 and has “output terminals” at sites 6, 8 and 9 – it is here that we will assess the response of the network. We first discuss what to expect based on the ideas above. This is then compared to the results of numerical simulations.

A cursory inspection tells us that this network is acyclic except for the subsystem (4,7). The finest decomposition that yields an acyclic quotient, then, is to regard each oscillator as a module except for (4,7), which must be grouped together as one. We choose, however, to work with a coarser decomposition, in which the (1,2,3,5,6)-subsystem is viewed as Module A, the (4,7)-subsystem as Module B, and the (8,9)-subsystem as Module C. Identifying the sites within each of these modules produces an acyclic quotient, as shown in Fig. 7(b).

Since Module B is the only module that is not itself acyclic and hence that is capable of generating unreliability, our results from Sect. 3 tell us that  $\lambda_{\max}$  for the entire network is  $\leq 0$  if and only

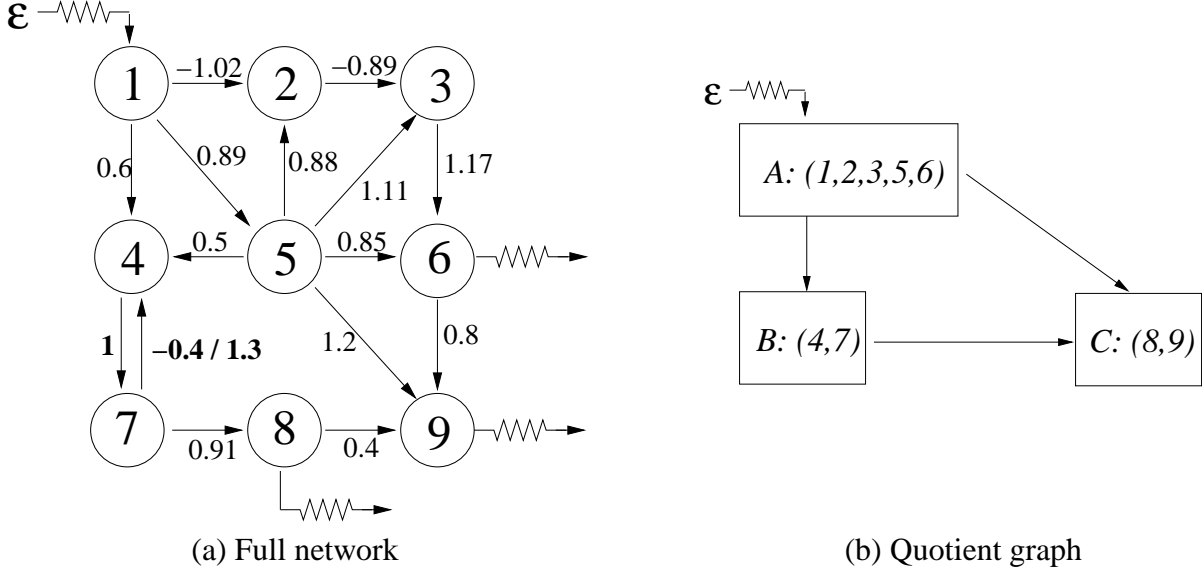


Figure 7: Example of a larger network and its quotient graph. In (a), we have labelled the edges with a sample of coupling constants. The  $\omega_i$  are drawn from  $[0.95, 1.05]$ .

if no unreliability is produced in Module B. In fact, since there are no freely rotating oscillators in the system, we expect  $\lambda_{\max}$  to be  $< 0$  if Module B behaves reliably. The behavior of Module B hinges a great deal on (i) the couplings  $a_{47}$  and  $a_{74}$ , which determine its reliability in isolation, and (ii) intrinsic network properties in the two Modules A and B together, especially when  $\epsilon$  is small; see Sects. 2 and 6. With regard to (i), the reliability profile of the 2-oscillator system compiled in [21] is handy. If unreliability is produced in Module B, then we expect to find sites 8 and 9 to be unreliable, with a lower reading of site entropy at site 9 than 8 due to the stabilizing effects of Module A; see Sect. 4. This is what general theory would lead one to predict.

We now present the results of simulations.

First we confirm that Module A alone is reliable as predicted:<sup>6</sup> In addition to the  $a_{ij}$  given in Fig. 7, we randomly drew coupling constants from  $\pm[0.8, 1.2]$  and frequencies  $\omega_i \in [0.95, 1.05]$ , and find that  $\lambda_{\max}$  for Module A ranges from roughly  $-0.3$  to  $-0.07$  when  $\epsilon = 1$ . Site distributions for the sites in Module A are, as predicted, well-localized. For a majority of parameters tested, 90% of an ensemble of  $10^4$  uniformly-chosen initial conditions has collapsed into a cube of side length  $\leq 10^{-2}$  after  $t=60-110$ ; in all our simulations, the ensemble collapses into a cube of side length  $\lesssim 10^{-7}$  after  $t \approx 1000$ . In particular, the “output terminal” at site 6 is always reliable.

Turning now to the reliability of Module B, we fixed the coupling constants as shown in Fig. 7, with  $\omega_i \in [0.95, 1.05]$  and  $\epsilon = 1$ , and ran simulations for the following two sets of parameters:

- (a)  $a_{47} = 1, a_{74} = -0.4$ : this case is predicted to be reliable
- (b)  $a_{47} = 1, a_{74} = 1.3$ : this case is predicted to be unreliable

<sup>6</sup>All Lyapunov exponents presented in this section have standard errors of  $\leq 0.004$  as estimated by the method of batched means. By the Central Limit Theorem, this means the actual  $\lambda_{\max}$  should lie within  $\approx 2.5 \times 0.004 = 0.01$  of the computed value with  $\gtrsim 99\%$  probability.

The predictions above are based on the behavior of the two-oscillator network “in isolation” (receiving white-noise stimulus of amplitude 1, see [21]), and on the results of Sect. 6. The following table summarizes the reliability properties of Module B, both in isolation and when embedded within the network:

### Module B Response

		<i>In isolation</i>	<i>Embedded in network</i>	
			$\varepsilon = 0$	$\varepsilon = 1$
(a)	$a_{47} = 1,$ $a_{74} = -0.4$	$\lambda_{\max} = -0.07$	$\lambda_{\max}^{fib} = 0.014$	$\lambda_{\max}^{fib} = -0.15$
(b)	$a_{47} = 1,$ $a_{74} = 1.3$	$\lambda_{\max} = 0.13$	$\lambda_{\max}^{fib} = 0.076$	$\lambda_{\max}^{fib} = 0.097$

Note that these values are consistent with the Proposal in Sect. 6: the behavior of the module at  $\varepsilon = 1$  when embedded within the network is effectively determined by its behavior in isolation. Furthermore, by Prop. 3.5, we know the Lyapunov exponent  $\lambda_{\max}$  of the *entire network* is equal to  $\lambda_{\max}^{fib}$  of Module B in case (b), and is  $\geq \lambda_{\max}^{fib}$  in case (a).

Finally, we study site distributions at sites 8 and 9. In case (a), we find again that computed site distributions are well localized. In case (b), we find the expected evidence of propagated unreliability and interference, with  $H(8) = -0.3$  and  $H(9) = -0.7$ .

In summary, the results of our simulations are entirely consistent with predictions based on the ideas developed in this paper.

## Conclusions

Understanding and predicting the reliability of responses for a general network is a daunting task. In this paper, we have limited ourselves to the simplest intrinsic dynamics, namely those of phase oscillators with pulsatile coupling. In this context, we believe we have raised and addressed a few basic issues for an interesting class of networks. Our main findings are:

1. *Acyclic networks, i.e., networks with a well defined direction of information flow, are*
  - (a) *never chaotic in the absence of inputs, and*
  - (b) *never unreliable when external stimuli are presented.*
2. *The mathematical analysis of the acyclic case can be extended to treat networks with a modular decomposition and acyclic quotient, i.e., networks for which the nodes can be grouped into modules, with inter-module connections being acyclic. These networks are fully capable of reliable and unreliable dynamics.*
3. *For networks with a nontrivial module decomposition, production of unreliability can be localized to specific modules, and is indicated by positive fiber Lyapunov exponents.*

4. *Once it is produced, unreliability will propagate: it can be attenuated but not completely removed; without intervention it actually grows for sites farther downstream.*
5. *There is evidence that the reliability of a module in isolation may give a good indication of its behavior when embedded in a larger network.* If true, this would simplify the analysis of networks that decompose into relatively simple modules with acyclic connections.

A general understanding of the issue in item 5 is not yet in sight, but our limited testing – using the 2-oscillator module studied in the companion paper [21] – produced encouraging results.

We hope that the findings above will be of some use in concrete applications in neuroscience and other fields.

**Acknowledgements:** K.L. and E.S-B. hold NSF Math. Sci. Postdoctoral Fellowships and E.S-B. a Burroughs-Wellcome Fund Career Award at the Scientific Interface; L-S.Y. is supported by a grant from the NSF.

## References

- [1] L. Arnold. *Random Dynamical Systems*. Springer, New York, 2003.
- [2] P.H. Baxendale. Stability and equilibrium properties of stochastic flows of diffeomorphisms. In *Progr. Probab.* 27. Birkhauser, 1992.
- [3] E. Brown, P. Holmes, and J. Moehlis. Globally coupled oscillator networks. In E. Kaplan, J.E. Marsden, and K.R. Sreenivasan, editors, *Problems and Perspectives in Nonlinear Science: A celebratory volume in honor of Lawrence Sirovich*, pages 183–215. Springer, New York, 2003.
- [4] J.-P. Eckmann and D. Ruelle. Ergodic theory of chaos and strange attractors. *Rev. Mod. Phys.*, 57:617–656, 1985.
- [5] B. Ermentrout. Neural networks as spatio-temporal pattern-forming systems. *Reports on Progress in Physics*, 61:353–430, 1991.
- [6] G. B. Ermentrout. Type I membranes, phase resetting curves, and synchrony. *Neural Comp.*, 8:979–1001, 1996.
- [7] G.B. Ermentrout and N. Kopell. Multiple pulse interactions and averaging in coupled neural oscillators. *J. Math. Biol.*, 29:195–217, 1991.
- [8] D. Goldobin and A. Pikovsky. Synchronization and desynchronization of self-sustained oscillators by common noise. *Phys. Rev. E*, 71:045201–045204, 2005.
- [9] D. Goldobin and A. Pikovsky. Antireliability of noise-driven neurons. *Phys. Rev. E*, 73:061906–1–061906–4, 2006.

- [10] J. Graczyk and G. Swiatek. Generic hyperbolicity in the logistic family. *Ann. Math.*, 146:1–52, 1997.
- [11] J. Guckenheimer. Isochrons and phaseless sets. *J. Math. Biol.*, 1:259–273, 1975.
- [12] J. Guckenheimer and P. Holmes. *Nonlinear Oscillations, Dynamical Systems, and Bifurcations of Vector Fields*. Springer-Verlag, 1983.
- [13] A.V. Herz and J.J. Hopfield. Earthquake cycles and neural reverberations: collective oscillations in systems with pulse-coupled threshold elements. *Phys. Rev. Lett.*, 75:1222–1225, 1995.
- [14] F.C. Hoppensteadt and E.M. Izhikevich. *Weakly Connected Neural Networks*. Springer-Verlag, New York, 1997.
- [15] M. Jakobson. Absolutely continuous invariant measures for one-parameter families of one-dimensional maps. *Comm. Math. Phys.*, 81:39–88, 1981.
- [16] Y. Le Jan. On isotropic Brownian motion. *Z. Wahr. Verw. Geb.*, 70:609–620, 1985.
- [17] E. Kosmidis and K. Pakdaman. Analysis of reliability in the Fitzhugh Nagumo neuron model. *J. Comp. Neurosci.*, 14:5–22, 2003.
- [18] L. F. Kozachenko and N. N. Leonenko. Sample estimate of the entropy of a random vector. *Problems of Information Transmission*, 23, 1987.
- [19] Y. Kuramoto. Phase- and center-manifold reductions for large populations of coupled oscillators with application to non-locally coupled systems. *Int. J. Bif. Chaos*, 7:789–805, 1997.
- [20] F. Ledrappier and L.-S. Young. Entropy formula for random transformations. *Probab. Th. and Rel. Fields*, 80:217–240, 1988.
- [21] K. Lin, E. Shea-Brown, and L-S. Young. Reliability of coupled oscillators I: Two oscillator systems. *submitted*, 2007.
- [22] K. Lin and L.-S. Young. Shear-induced chaos. *arXiv:0705.3294v1* [math.DS], 2007.
- [23] M. Lyubich. Regular and stochastic dynamics in the real quadratic family. *PNAS*, 95:14025–14027, 1998.
- [24] P. Mattila. *Geometry of sets and measures in Euclidean space*. Cambridge University Press, 1995.
- [25] H. Nakao, K. Arai, K. Nagai, Y. Tsubo, and Y. Kuramoto. Synchrony of limit-cycle oscillators induced by random external impulses. *Physical Review E*, 72:026220–1 – 026220–13, 2005.
- [26] D. Nualart. *The Malliavin Calculus and Related Topics*. Springer-Verlag, 2006.

- [27] A.M. Nunes and Pereira. J.V. Phase-locking of two Andronov clocks with a general interaction. *Phys. Lett. A*, 107:362–366, 1985.
- [28] K. Pakdaman and D. Mestivier. External noise synchronizes forced oscillators. *Phys. Rev. E*, 64:030901–030904, 2001.
- [29] C.S. Peskin. *Mathematical Aspects of Heart Physiology*. Courant Institute of Mathematical Sciences, New York, 1988.
- [30] A. Pikovsky, M. Rosenblum, and J. Kurths. *Synchronization: A Universal Concept in Non-linear Sciences*. Cambridge University Press, Cambridge, 2001.
- [31] O.V. Popovych, Y.L. Maistrenko, and P.A. Tass. Phase chaos in coupled oscillators. *Phys. Rev. E*, 71:065201–1 – 065201–4, 2005.
- [32] J. Rinzel and G.B. Ermentrout. Analysis of neural excitability and oscillations. In C. Koch and I. Segev, editors, *Methods in Neuronal Modeling*, pages 251–291. MIT Press, 1998.
- [33] J. Ritt. Evaluation of entrainment of a nonlinear neural oscillator to white noise. *Phys. Rev. E*, 68:041915–041921, 2003.
- [34] S. Strogatz. From Kuramoto to Crawford: Exploring the onset of synchronization in populations of coupled oscillators. *Physica D*, 143:1–20, 2000.
- [35] S. Strogatz and R. Mirollo. Synchronization of pulse-coupled biological oscillators. *SIAM Journal on Applied Mathematics*, 50:1645 – 1662, 1990.
- [36] J. Teramae and T. Fukai. Reliability of temporal coding on pulse-coupled networks of oscillators. *arXiv:0708.0862v1 [nlin.AO]*, 2007.
- [37] J. Teramae and D. Tanaka. Robustness of the noise-induced phase synchronization in a general class of limit cycle oscillators. *Phys. Rev. Lett.*, 93:204103–204106, 2004.
- [38] J. D. Victor. Binless strategies for estimation of information from neural data. *Physical Review E*, 66, 2002.
- [39] Q. Wang and L.-S. Young. From invariant curves to strange attractors. *Comm. Math. Phys.*, 225:275–304, 2002.
- [40] Q. Wang and L.-S. Young. Strange attractors in periodically-kicked limit cycles and Hopf bifurcations. *Comm. Math. Phys.*, 240:509–529, 2003.
- [41] A. Winfree. Patterns of phase compromise in biological cycles. *J. Math. Biol.*, 1:73–95, 1974.
- [42] A. Winfree. *The Geometry of Biological Time*. Springer, New York, 2001.

- [43] L.-S. Young. Ergodic theory of differentiable dynamical systems. In *Real and Complex Dynamics*, NATO ASI Series, pages 293–336. Kluwer Academic Publishers, 1995.
- [44] L.-S. Young. What are SRB measures, and which dynamical systems have them? *Journal of Statistical Physics*, 108(5):733–754, 2002.
- [45] C. Zhou and J. Kurths. Noise-induced synchronization and coherence resonance of a Hodgkin-Huxley model of thermally sensitive neurons. *Chaos*, 13:401–409, 2003.